ELSEVIER

Journal of Quantitative Spectroscopy & Radiative Transfer 100 (2006) 91–102

Journal of Quantitative Spectroscopy & Radiative Transfer

www.elsevier.com/locate/jqsrt

# Scattering phase functions of horizontally oriented hexagonal ice crystals

Guang Chen[a], Ping Yang[a,*], George W. Kattawar[b], Michael I. Mishchenko[c]

[a]*Department of Atmospheric Sciences, Texas A&M University, College Station, TX 77843, USA*
[b]*Department of Physics, Texas A&M University, College Station, TX 77843, USA*
[c]*NASA Goddard Institute for Space Studies, 2880 Broadway, New York, NY 10025, USA*

**Abstract**

Finite-difference time domain (FDTD) solutions are first compared with the corresponding *T*-matrix results for light scattering by circular cylinders with specific orientations. The FDTD method is then utilized to study the scattering properties of horizontally oriented hexagonal ice plates at two wavelengths, 0.55 and 12 μm. The phase functions of horizontally oriented ice plates deviate substantially from their counterparts obtained for randomly oriented particles. Furthermore, we compute the phase functions of horizontally oriented ice crystal columns by using the FDTD method along with two schemes for averaging over the particle orientations. It is shown that the phase functions of hexagonal ice columns with horizontal orientations are not sensitive to the rotation about the principal axes of the particles. Moreover, hexagonal ice crystals and circular cylindrical ice particles have similar optical properties, particularly, at a strongly absorbing wavelength, if the two particle geometries have the same length and aspect ratio defined as the ratio of the radius or semi-width of the cross section of a particle to its length. The phase functions for the two particle geometries are slightly different in the case of weakly absorbing plates with large aspect ratios. However, the solutions for circular cylinders agree well with their counterparts for hexagonal columns.


*Keywords:* FDTD; T-matrix; Phase matrix; Horizontal orientation; Hexagon; Cylinder

## 1. Introduction

To understand the terrestrial climate system and its evolution better, it is essential to know the radiative properties of cirrus clouds since the latter cover more than 20% of the globe [1–4]. The pristine ice crystals within cirrus clouds have hexagonal structures, which are associated with various optical phenomena in the atmosphere [5]. In addition to the nonspherical effect of ice crystals, the orientations of these particles are also important to their optical properties. In the atmosphere, large ice crystals tend to have their longest dimension oriented horizontally, as demonstrated by Platt [6] using lidar measurements for ice plates. Stephens [7] demonstrated the importance of the shapes and orientations of nonspherical particles in radiative transfer calculations. While the errors associated with the neglect of nonsphereicity of ice crystals in dealing with cirrus

*Corresponding author. Tel.: +1 979 845 4923.
*E-mail address:* pyang@ariel.met.tamu.edu (P. Yang).

0022-4073/$ - see front matter © 2005 Elsevier Ltd. All rights reserved.
doi:10.1016/j.jqsrt.2005.11.029

radiative properties can be substantial, the influence of the specific orientations of the long cylinders on cloud albedo, absorption, and emission can also be significant in comparison with the case for randomly oriented ice crystals. Therefore, the scattering properties of oriented crystals should be characterized as functions of both the zenith and azimuthal angles of the incident and scattered light. Rockwitz [8] and Takano and Liou [9] have previously discussed the scattering properties of horizontally oriented ice crystals using the ray-tracing method. Note that a new approach based on a combination of the ray-tracing technique with diffraction on flat facets has been recently suggested by Hesse and Ulanowski [10] for the scattering of light by long prisms. The single-scattering properties of oriented particles have also been discussed by Mishchenko et al. [11] and by Havemann and Baran [12] using the rigorous $T$-matrix method [13,14].

In this study, we first compare the solutions for the phase matrix based on the finite-difference time domain (FDTD) [15–18] and the $T$-matrix methods [11–14] assuming oriented circular cylinders. The phase matrix elements $P_{11}$, $P_{12}/P_{11}$, $P_{33}/P_{11}$ and $P_{34}/P_{11}$ from the two methods are compared at wavelengths of 0.55 and 12 μm. Furthermore, we applied the FDTD method to the scattering of light by horizontally oriented hexagonal particles using several different schemes to average over the particle orientation. Note that horizontally oriented particles, for example, columns can have arbitrary orientations with one degree of freedom (hereafter, 1D freedom) in terms of the arbitrary orientations of their principal axes in horizontal planes, or, with two degrees of freedom (hereafter, 2D freedom) for the case where the particles' principal axes can be arbitrarily oriented in horizontal planes while at the same time the particles can also randomly rotate about their axes. Therefore, the resultant anisotropic phase functions depend on scattering zenith angle and also on the azimuthal angle of the scattering plane of interest. Lee et al. [19] investigated the feasibility of using circular cylinders as surrogates for randomly oriented hexagonal ice crystals in the computation of the scattering properties of the latter. In this study, we investigated the feasibility and errors associated with using circular cylinders as surrogates for hexagonal columns or plates in computing the optical properties of

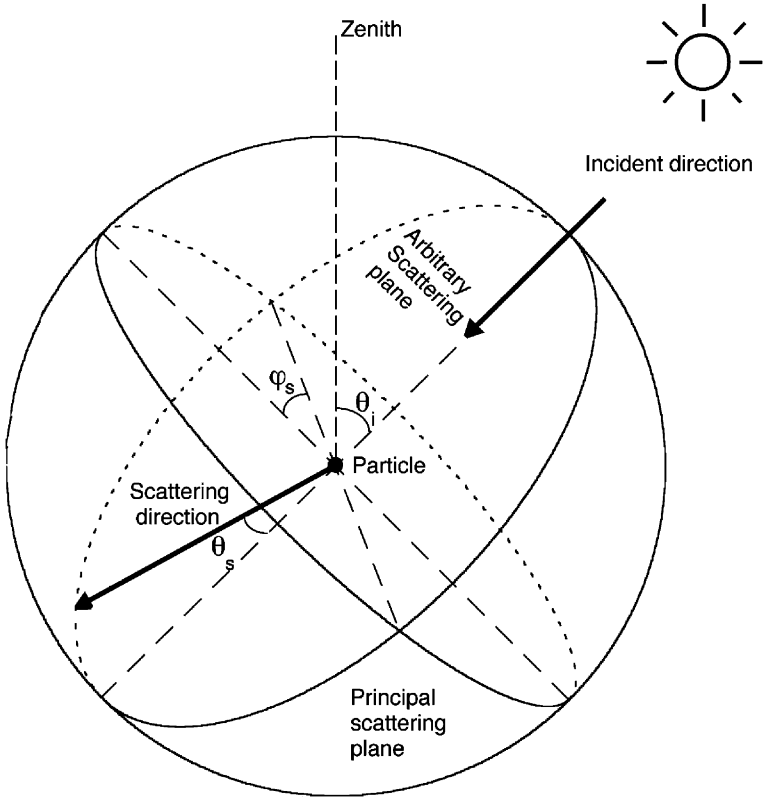


Fig. 1. Geometry of light scattering.

horizontally oriented ice crystals. The *T*-matrix method [11–14] is used to calculate the scattering properties of circular cylinders.

## 2. Definitions

Two geometries, circular cylinders and hexagonal prisms are considered in this study. A circular cylinder is specified in terms of the radius of its cross section ($r$) and length ($L$). A hexagonal prism is defined in terms of its side length ($a$, which is also the radius of the corresponding circumscribed cylinder) and principal axis length ($L$). Aspect ratios for these particles are defined as $r/L$ for circular cylinders and $a/L$ for hexagonal prisms. The size parameters of these particles are defined as $k$ (the wave number $= 2/\lambda$) multiplied by the largest dimensions of the particles, where $\lambda$ is the incident wavelength. When $L$ is larger than $2r$ or $2a$, size parameters are defined as $kL$; otherwise, size parameters are defined as $ka$ or $kr$.

In this study, we use six angles, $\varphi_p$, $\theta_p$, $\psi_p$, $\theta_i$, $\theta_s$, and $\varphi_s$, to specify the incident-scattering configuration for oriented particles. Consider the scattering of sunlight by ice crystals in the atmosphere. As shown in Fig. 1, the incident angle with respect to the zenith direction is denoted by $\theta_i$. For scattering particles with horizontal orientations, their scattering matrices depend on both the scattering angle ($\theta_s$) and the azimuthal angle ($\varphi_s$) of a scattering plane to which the scattering properties are referenced. The principal scattering plane, the plane with $\varphi_s = 0$, contains both the zenith and incident directions, i.e., the principal plane is a vertical plane in this case. An interesting point to note is that some oriented particles (e.g., circular plates with vertical orientation of their symmetric axes) are symmetric with respect to mirroring about the principal plane. This symmetry leads to some unique features of the scattering properties of the particles, as we will demonstrate in Section 3.

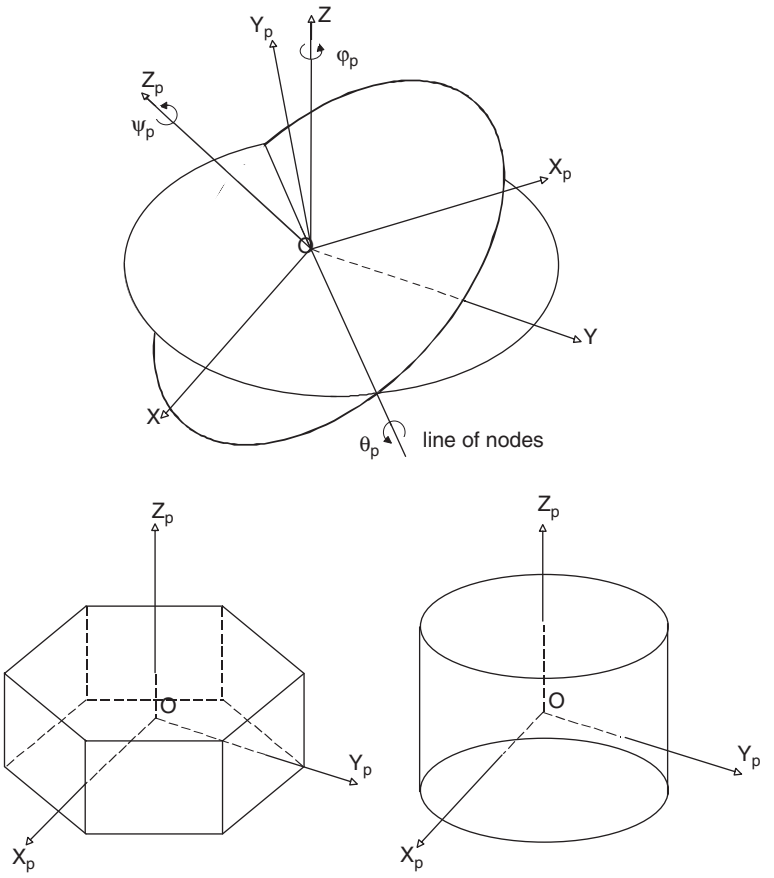


Fig. 2. Definition of the Euler angles and orientations of geometries of hexagonal column and cylinder in the particle coordinate system.

In the present numerical computation, we define a laboratory coordinate system, $OXYZ$, and a particle coordinate system, $OX_pY_pZ_p$. The particle system is fixed to the corresponding scattering particle and rotates with the particle. The relative orientation of the particle coordinate system with respect to the laboratory system is specified by three Euler angles, $\varphi_p$, $\theta_p$ and $\psi_p$ where $\varphi_p \in [0, 2\pi]$ indicates a counterclockwise rotation about the $Z$-axis, $\theta_p \in [0, \pi]$ indicates a rotation about the line of nodes, and $\psi_p \in [0, 2\pi]$ indicates a rotation about the $Z$-axis of the particle coordinate system, as shown in the upper panel of Fig. 2. Note that, to define the particle system, the rotations specified by the three Euler angles are sequentially given by the three noncommutative angles, $\varphi_p$, $\theta_p$ and $\psi_p$. The lower panels of Fig. 2 show the geometries of a hexagon and a circular cylinder in the particle system.

As described by Platt [6], ice plates ($L<2a$) or columns ($L>2a$) in ice clouds prefer to have their longest dimension oriented horizontally. In this case, the corresponding phase matrix elements are functions of scattering zenith angle, $\theta_s$, and azimuthal angle, $\varphi_s$. In this study, three schemes are used for averaging over particles' orientations that can be arbitrary but confined to be horizontal for computing the scattering properties of hexagonal particles. As shown in the Fig. 3, hexagonal plates can have random rotational angles about their symmetry axes which are their principal axes oriented vertically. In the present computation of the scattering properties of hexagonal plates, 120 orientations with the rotation angles from $0^\circ$ to $360^\circ$ with a resolution of $3^\circ$ are used. Hexagonal columns can have orientations with 1D or 2D freedom. For the horizontal orientations with 1D freedom, the particles can have arbitrary rotation about the $Z$-axis. The number of orientations assumed for the present computation is 18 with a resolution of $20^\circ$ for the rotation

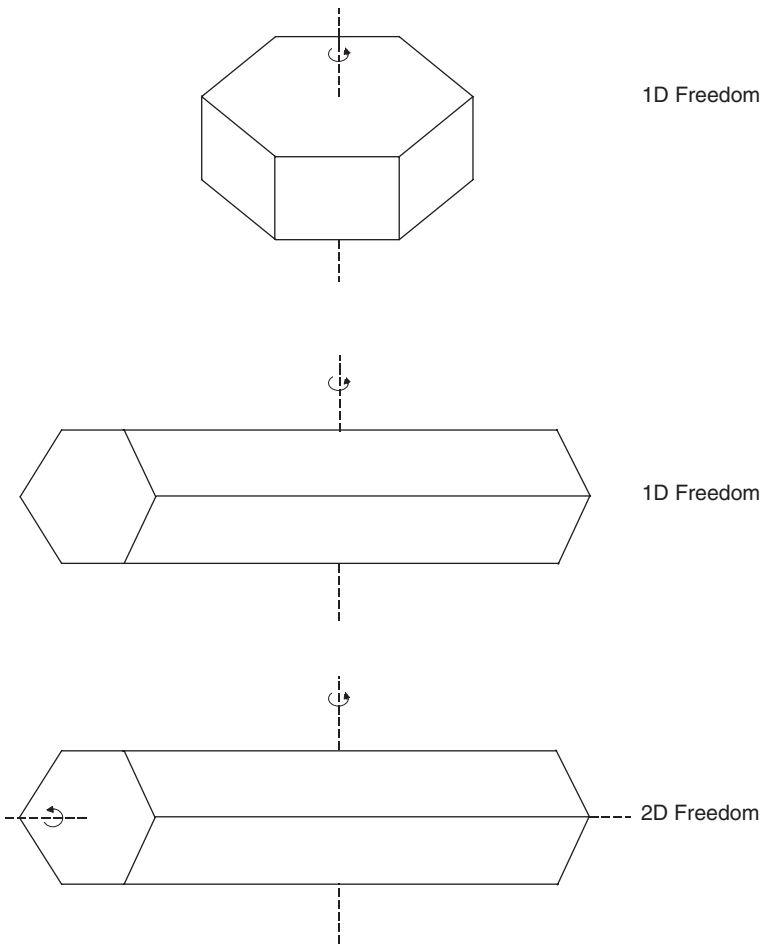


Fig. 3. Orientation-averaging schemes for hexagonal plates and columns.

about the $Z$-axis from 0° to 360°. For the random orientations with 2D freedom, the columns not only rotate horizontally about the $Z$-axis but also rotate about their symmetry axes. In this case, the orientation resolution is $18 \times 24$, where 18 indicates the number of rotations about the $Z$-axis and 24 indicates the number of rotations about the principal axis (with a resolution of 15°). In this study, the scattering properties of horizontally oriented particles are also compared with those of 3D randomly oriented particles. For the 3D randomly oriented particles, $24 \times 18 \times 360$ orientations are accounted for, where 24 is the number of the

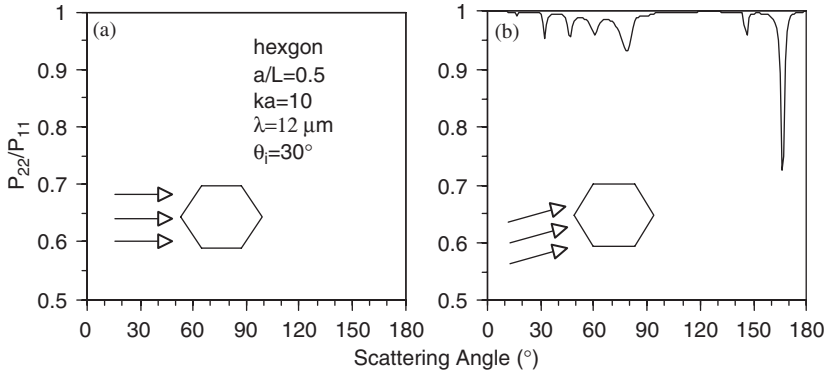


Fig. 4. Phase matrix element ratio $P_{22}/P_{11}$ of a fixed oriented ice hexagonal column with a unit aspect ratio at a wavelength of 12 μm at an incident angle of 30°.

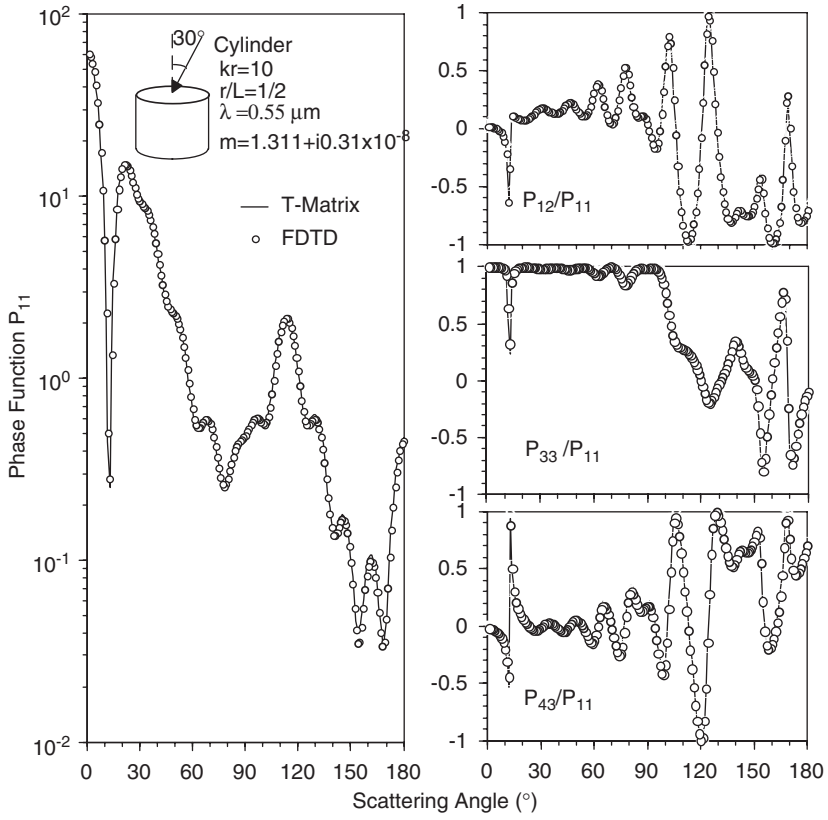


Fig. 5. Phase matrix element ratios $P_{11}$, $P_{12}/P_{11}$, $P_{33}/P_{11}$ and $P_{34}/P_{11}$ of a fixed oriented ice cylinder with a unit aspect ratio at a wavelength of 0.55 μm at an incident angle of 30°.

incident azimuth angles, 18 is the number of the incident zenith angles, and 360 is the number of the scattering azimuth angles. We find little improvement on the accuracy of the results, if the angular resolution for averaging the particle orientations increases further. The mean phase matrix averaged for particle orientations can be written as follows:

$$\langle P(\theta_s,\varphi_s)\rangle = \frac{\int_{\varphi_1}^{\varphi_2} d\varphi_p \int_{\theta_1}^{\theta_2} \sin\theta_p \, d\theta_p \int_{\psi_1}^{\psi_2} P(\varphi_p,\theta_p,\psi_p,\theta_s,\varphi_s) C_{sca}(\varphi_p,\theta_p,\psi_p,\theta_s,\varphi_s)\, d\psi_p}{\int_{\varphi_1}^{\varphi_2} d\varphi_p \int_{\theta_1}^{\theta_2} \sin\theta_p \, d\theta_p \int_{\psi_1}^{\psi_2} C_{sca}(\varphi_p,\theta_p,\psi_p,\theta_s,\varphi_s)\, d\psi_p}, \quad (1)$$

where $P(\varphi_p,\theta_p,\psi_p,\theta_s,\varphi_s)$ and $C_{sca}(\varphi_p,\theta_p,\psi_p,\theta_s,\varphi_s)$ are the phase matrix and the scattering cross section for one specific orientation, respectively.

In the FDTD method the grid resolution specified in terms of $n = \lambda/\Delta s$, where $\lambda$ is the incident wavelength and $\Delta s$ is the length of a grid cell, is a key parameter that determines the accuracy of the numerical solutions and the corresponding computational effort. In this study, we select $n = 25m_r$, in which $m_r$ is the real part of the refractive index of the particle. However, for a case associated with a large aspect ratio, a finer grid resolution is normally necessary to obtain an accurate FDTD solution. For example, $n$ is taken as 60 for an aspect ratio of 1/6 in the present study.

## 3. Validation of the FDTD method for oriented particles

The FDTD and $T$-matrix methods are used to compute the phase matrices for a circular cylinder with a unit aspect ratio and a fixed orientation at wavelengths of 12 and 0.55 μm. The complex refractive indices of ice at these two wavelengths are (1.2799, 0.4133) and (1.311, $0.311 \times 10^{-8}$) taken from the data sets of Warren [20]. As shown in the left panel at the bottom of the Fig. 2, in the laboratory coordinate system, the $Z$-axis is

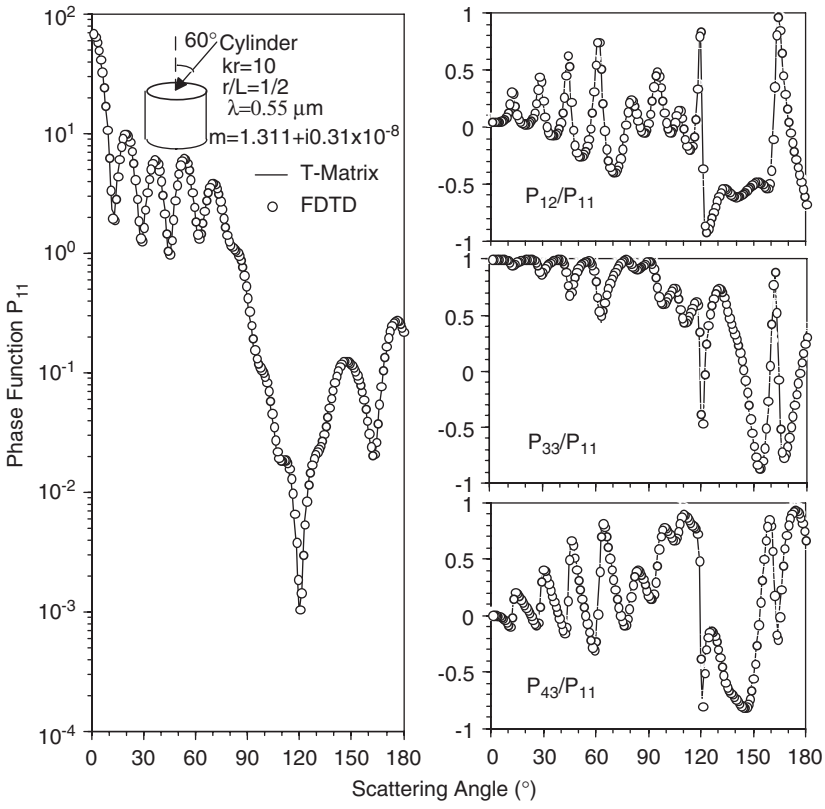


Fig. 6. Phase matrix element ratios $P_{11}$, $P_{12}/P_{11}$, $P_{33}/P_{11}$ and $P_{34}/P_{11}$ of a fixed oriented ice cylinder with a unit aspect ratio at a wavelength of 0.55 μm at an incident angle of 60°.

defined as the symmetry axis of the ice cylinder. The solutions are compared for a scattering azimuth angle, $\varphi_s$, of 0°, and two incident angles, 30° and 60°. According to the discussion in the preceding section, we notice that at a scattering azimuth angle of 0°, the scattering plane coincides with the principal plane of the cylinder. If a particle has a mirror symmetry relative to the principal plane, then the signs of $S_3$ and $S_4$ change for the mirror particle. We can think of the complete particle as consisting of two halves which are touching and when we sum the scattering amplitude matrix in this case, only $S_1$ and $S_2$ survive. Consequently, in the corresponding phase matrix, elements of $P_{13}$, $P_{14}$, $P_{23}$, $P_{24}$, $P_{31}$, $P_{32}$, $P_{41}$ and $P_{42}$ are zero, and $P_{22}/P_{11}$ is unity. It should be noted that the deviation of $P_{22}/P_{11}$ from unity has normally been regarded as an indication of the nonsphericity of a scattering particle [13,21]; however, we have shown that making a measurement in the principal plane of a particle which has mirror symmetry about this plane will "look spherical".

Fig. 4 shows the phase matrix element, $P_{22}/P_{11}$, for a fixed oriented hexagonal column at a wavelength of 12 μm and an incident angle of 30°. Evidently, $P_{22}/P_{11}$ is unity when the incident azimuth angle is zero (panel (a) of Fig. 4) since it is in a plane of mirror symmetry of the particle. However, $P_{22}/P_{11}$ is a function of the scattering zenith angle at an incident azimuth angle of 15° (panel (b) of Fig. 4). It should also be noted that $P_{12} = P_{21}$, $P_{33} = P_{44}$ and $P_{43} = -P_{34}$. In the following $P_{11}$, $P_{12}/P_{11}$, $P_{33}/P_{11}$ and $P_{34}/P_{11}$ will be discussed.

Fig. 5 shows the phase matrix elements $P_{11}$, $P_{12}/P_{11}$, $P_{33}/P_{11}$ and $P_{34}/P_{11}$ of a circular cylinder at a wavelength of 0.55 μm and an incident angle of 30°. It is evident that the FDTD solution agrees well with that from the $T$-matrix results at all scattering angles. For $P_{11}$, solutions are sightly different for angles near 150°. For $P_{12}/P_{11}$ and $P_{43}/P_{11}$, the FDTD and $T$-matrix results are essentially the same. For $P_{33}/P_{11}$, excellent agreement of the two solutions is also noticed except for slight differences near 150°.

Fig. 6 is the same as Fig. 5 except for an incident angle of 60°. In this case, the FDTD solutions essentially converge to the $T$-matrix results in terms of the phase function P11. For the other three phase matrix elements,

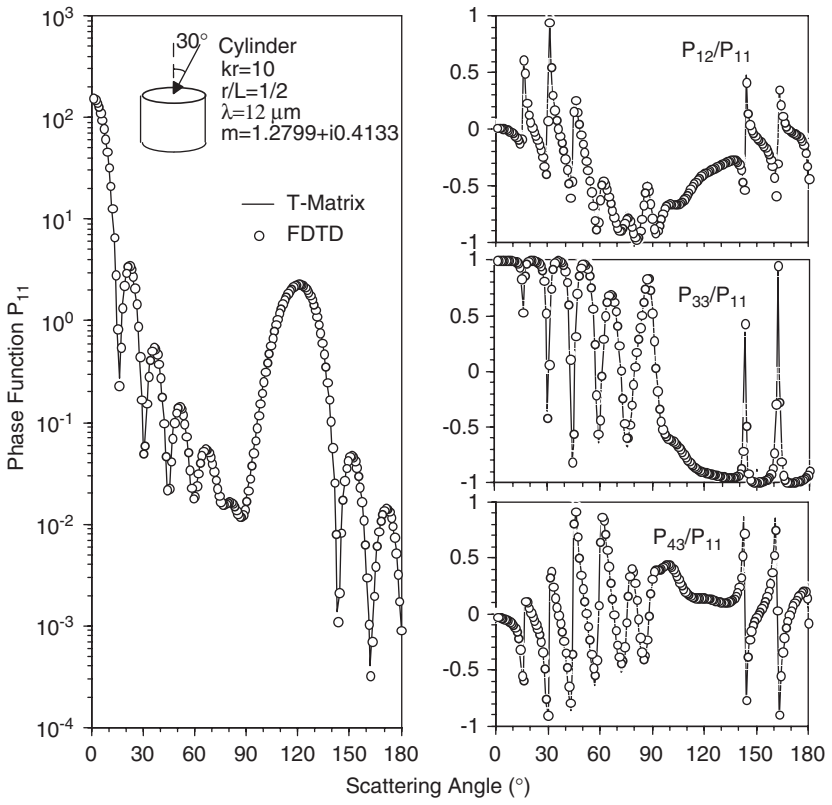


Fig. 7. Phase matrix element ratios $P_{11}$, $P_{12}/P_{11}$, $P_{33}/P_{11}$ and $P_{34}/P_{11}$of a fixed oriented ice cylinder with a unit aspect ratio at a wavelength of 12 μm at an incident angle of 30°.

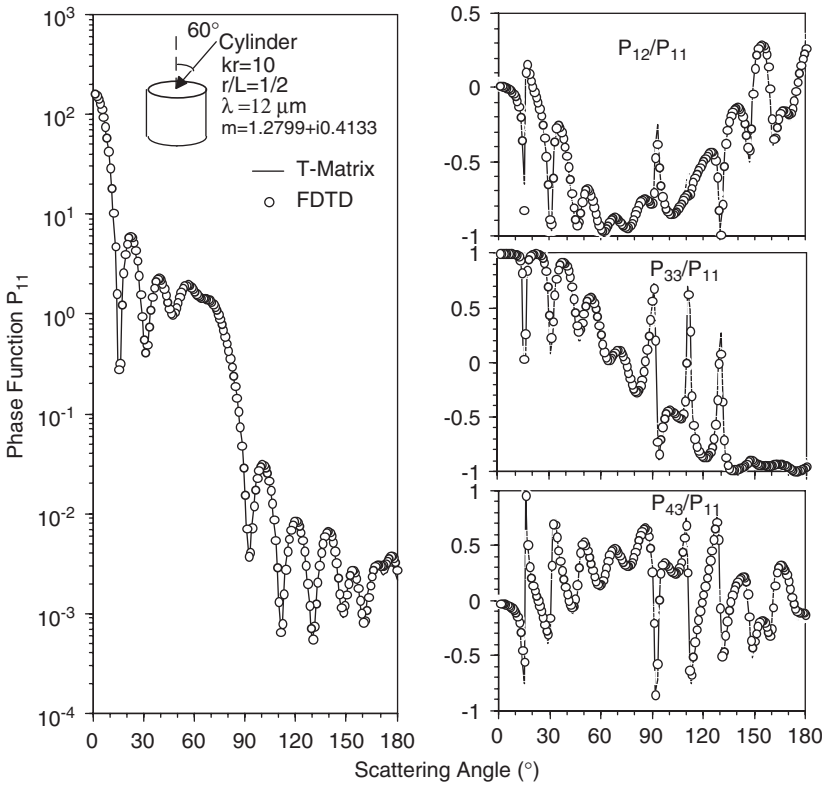


Fig. 8. Phase matrix element ratios $P_{11}$, $P_{12}/P_{11}$, $P_{33}/P_{11}$ and $P_{34}/P_{11}$ of a fixed oriented ice cylinder with a unit aspect ratio at a wavelength of 12 μm at an incident angle of 60°.

the FDTD solutions also agree with $T$-matrix calculations, except for $P_{43}/P_{11}$ at 120° and 165° where the minima in these two quantities occur.

Figs. 7 and 8 are the same as Figs. 5 and 6, respectively, except that a wavelength of 12 μm is used for the two results reported in Figs. 7 and 8. At 12 μm wavelength, ice is quite absorptive as the imaginary part of the refractive index is 0.4133. Again, the FDTD solutions agree well with the $T$-matrix solutions except at some scattering angles where the maxima or minima of the phase matrix elements occur, particularly in the case when the incident angle is 30° (Fig. 7). Baran et al. [22] have also compared the solutions to the scattering of light by nonspherical ice crystals computed from the $T$-matrix and FDTD methods for the case of random orientations at nonabsorbing and absorbing wavelengths.

## 4. Single-scattering properties of horizontally oriented hexagonal ice crystals and circular cylinders

The phase functions for horizontally oriented hexagonal ice plates with an aspect ratio of $a/L = 2$ are computed with the FDTD method on the basis of the previously described 1D-freedom scheme for averaging over the particle's horizontal orientations. The numerical computations are carried out at wavelengths of 0.55 and 12 μm with three incident angles, 0°, 30°, and 60°. Fig. 9 shows the variations of phase functions of both hexagonal and cylindrical ice plates versus the scattering zenith and azimuth angles. Overall, the phase functions for the two particle geometries are quite similar. An interesting feature associated with the phase functions is the scattering maxima observed at $\theta_s = 120°$ and $\varphi_s = 90°$. These maxima are caused by the external reflection associated with the top face of ice plates which is the genesis for "sunpillars".

Fig. 10 shows phase functions of horizontally oriented hexagonal columns with an aspect ratio of $a/L = 1/6$ for two incident angles, 30° and 60°. The solutions on the basis of the previously described 1D- and 2D-freedom orientation averaging schemes are shown in the first and second rows of Fig. 10, respectively. The

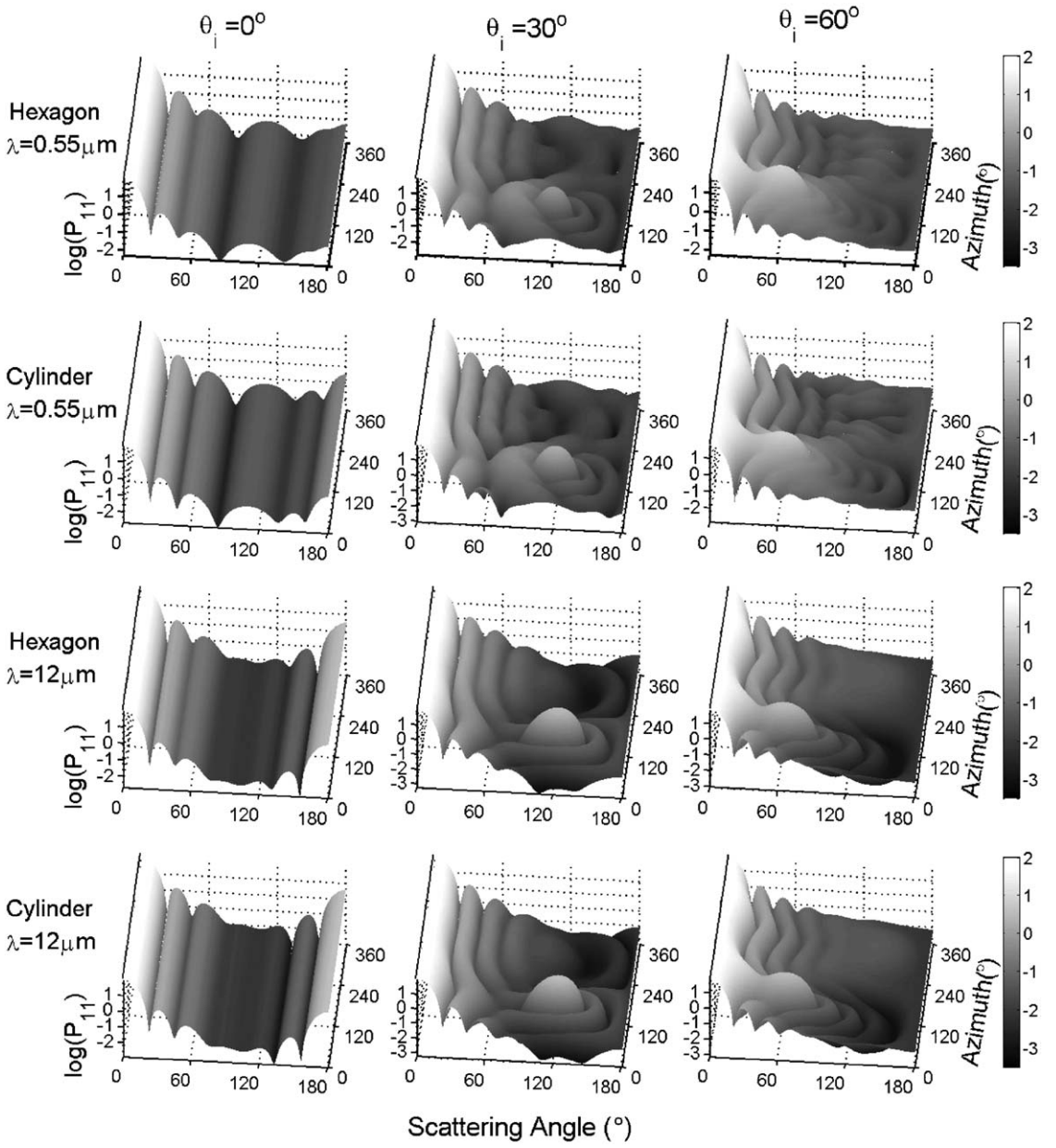


Fig. 9. Phase functions of horizontally oriented hexagonal plates and their equivalent cylinder plates with an aspect ratio of 0.25 at wavelengths of 12 and 0.55 μm.

third row shows the phase functions of horizontally oriented circular ice cylinders. As a circular cylinder is rotationally symmetric about it principal axis, only 1D-freedom orientation average is required. Reflection peaks caused by the external reflection from the column side faces are not significant when compared to the case for horizontally oriented plates. A comparison of the results in the first and second rows of Fig. 10 indicates that at the scattering angles between 0°and 60°, the hexagonal columns with the two orientation-averaging schemes have similar optical properties, and the relative differences due to the two different orientation-averaging schemes are less than 10%. At the other scattering angles, only slight differences are noticed. Therefore, the rotation about the principal axes of the columns does not have a significant influence on the mean phase functions.

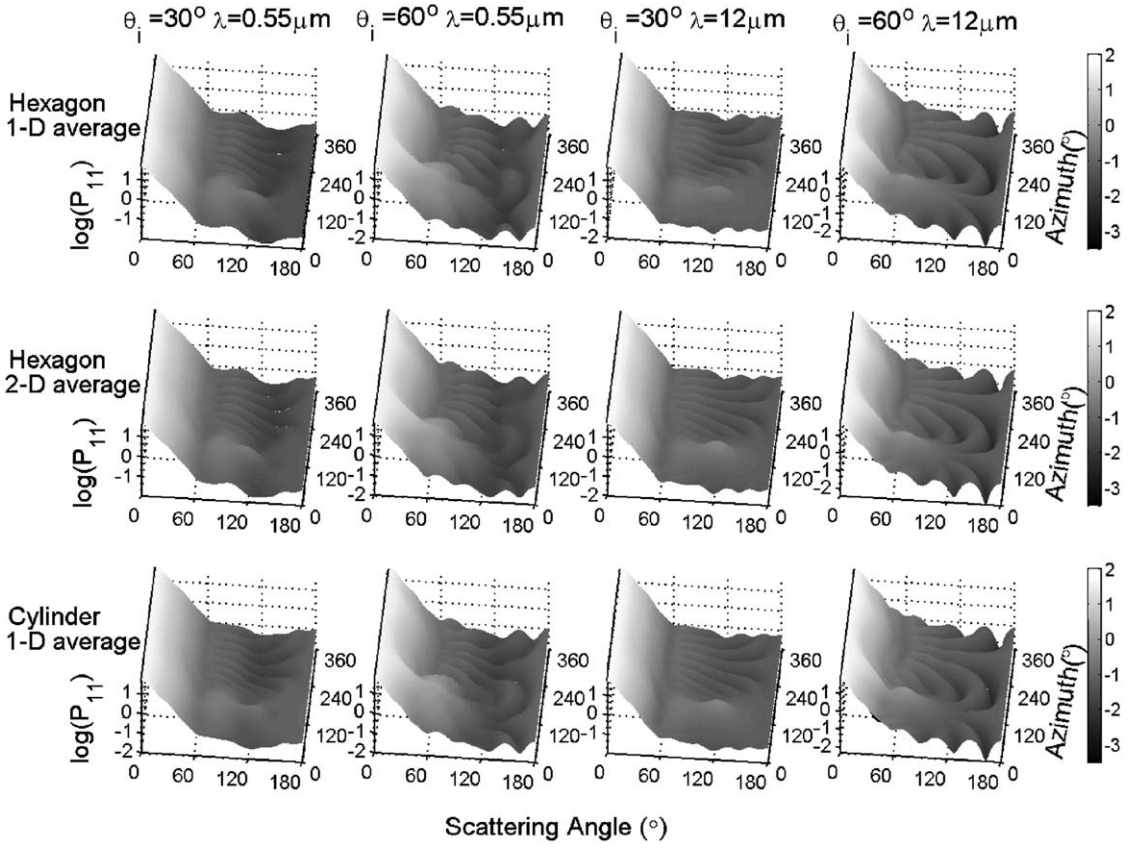


Fig. 10. Phase functions of horizontally oriented hexagonal columns and their equivalent cylinders with an aspect ratio of 3 at wavelengths of 12 and 0.55 μm.

Circular cylinders have been suggested as surrogates for hexagonal ice crystals in the literature. For example, Lee et al. [19] noticed that circular cylinders have similar scattering and absorption properties as hexagonal ice crystals when a random orientation condition is imposed at the infrared wavelengths. The results shown in Figs. 9 and 10 indicate that circular cylinders can also be used as surrogates for hexagonal ice crystals even if horizontal orientations are considered. At the two wavelengths of 12 and 0.55 μm, the relative differences between the equivalent cylinder and the hexagonal plate are less than 4% in the forward direction and are less than 10% in the backward direction for all tilted incident cases. Therefore, a circular cylinder can be used as a surrogate for a horizontally oriented hexagonal plate in the computation of its scattering properties, provided the size parameter is not inordinately large.

Fig. 11 shows the comparison of the phase functions for 1D horizontally and 3D randomly oriented ice crystals. An incident angle of 0° is used for the computation for the horizontally oriented particles. The randomly oriented results are substantially different from the horizontally oriented solutions. Particularly, for the strong absorption case, the back scattering of horizontally oriented plates caused by the external reflections is approximately 50 times that for the randomly oriented particle.

## 6. Conclusions

We compared the performance of the FDTD method with that of the *T*-matrix method for the computation of the scattering properties of oriented nonspherical particles. Three numerical schemes were used to average the particle horizontal orientations for hexagonal plates and columns. The corresponding solutions for random orientations were also calculated by using the FDTD method. It was found that the phase functions for horizontally oriented hexagonal plates are sensitive to the scattering azimuthal angle, and are substantially

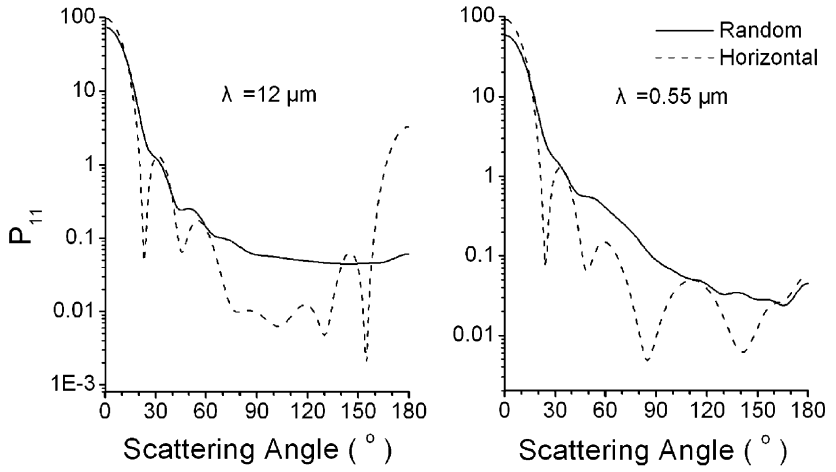


Fig. 11. Normalized phase functions of randomly oriented and horizontally oriented ($\theta_i = 0°$) ice hexagonal plates with an aspect ratio of 0.25 at 12 and 0.55 μm wavelengths.

different from the randomly oriented results. The phase functions of the equivalent cylinders agreed well with the corresponding counterparts of hexagonal ice crystals at all incident angles at a wavelength of 12 μm. At a wavelength of 0.55 μm, some discrepancies were noted at the scattering angles when the reflection peaks for the horizontal oriented plates occur. The comparisons of phase functions for the hexagonal columns with 1D- and 2D-freedom orientation-averaging schemes indicated that the results are not sensitive to the rotation of the particles about their principal axes. It was also noted that the equivalent circular cylinders can be applied as surrogates for hexagonal columns even when the particles are horizontally oriented.

## Acknowledgements

Ping Yang acknowledges support from the National Science Foundation (ATM-0239605) and the NASA Radiation Sciences Program (NNG04GL24G). George Kattawar acknowledges support from the Office of Naval Research (N00014-02-1-0478). Michael Mishchenko acknowledges support from the NASA Radiation Sciences Program and the NASA Glory Mission Project.

## References

[1] Donner L, Seman CJ, Sden BJ, Hemler RS, Warren JC, Strom J, et al. Large-scale ice clouds in the GFDL SKYHI general circulation model. J Geophys Res 1997;102:21745–68.
[2] Liou KN, Takano Y. Light scattering by nonspherical particles: remote sensing and climatic implications. Atmos Res 1994;31: 271–98.
[3] Liou KN. Influence of cirrus clouds on weather and climate processes: a global perspective. Mon Weather Rev 1986;114:1167–99.
[4] Hartmann DL, Ockert-Bell ME, Michelsen ML. The effect of cloud type on earth's energy balance: global analysis. J Climate 1992;5:1281–304.
[5] Greenler R. Rainbows, halos, and glories. Cambridge, UK: Cambridge University Press; 1980.
[6] Platt CMR. Lidar backscatter from horizontal ice crystal patterns. J Appl Meteorol 1978;17:482–8.
[7] Stephens GL. Radiative transfer on a linear lattice: application to anisotropic ice crystal clouds. J Atmos Sci 1980;37:2095–104.
[8] Rockwitz KD. Scattering properties of horizontally oriented ice crystal columns in cirrus clouds: Part 1. Appl Opt 1989;28:4103–10.
[9] Takano Y, Liou KN. Solar radiative transfer in cirrus clouds. Part I: cingle-ccattering and optical properties of hexagonal ice crystals. J Atmos Sci 1989;46:3–19.
[10] Hesse E, Ulanowski Z. Scattering from long prisms computed using ray tracing combined with diffraction on facets. JQSRT 2003:721–32.
[11] Mishchenko MI, Wielaard DJ, Carlson BE. *T*-matrix computations of zenith-enhanced lidar backscatter from horizontally oriented ice plates. Geophys Res Lett 2000;39:1026–31.
[12] Havemann S, Baran AJ. Extension of *T*-matrix to scattering of electromagnetic plane waves by non-axisymmetric dielectric particles: application to hexagonal ice cylinders. JQSRT 2001;70:139–58.

[13] Waterman PC. Symmetry, unitarity, and geometry in electromagnetic scattering. Phys Rev D 1971;3:1953–69.
[14] Mishchenko MI, Travis LD, Lacis AA. Scattering, absorption, and emission of light by small particles. Cambridge: Cambridge University Press; 2002.
[15] Yee SK. Numerical solution of initial boundary value problems involving Maxwell's equations in isotropic media. IEEE Trans Antennas Propag 1966;14:302–7.
[16] Taflove A. Computational electrodynamics: the finite-difference time-domain method. Boston, MA: Artech House; 1995.
[17] Yang P, Liou KN. Finite-difference time domain method for light scattering by small ice crystals in three-dimensional space. J Opt Soc Am A 1996;13:2072–85.
[18] Sun W, Fu Q, Chen Z. Finite-difference time-domain solution of light scattering by dielectric particles with perfectly matched layer absorbing boundary conditions. Appl Opt 1999;38:3141–51.
[19] Lee YK, Yang P, Mishchenko MI, Baum BA, Hu Y, Huang H-L, et al. On the use of circular cylinders as surrogates for hexagonal pristine ice crystals in scattering calculations at infrared wavelengths. Appl Opt 2003;42:2653–64.
[20] Warren S. Optical constants of ice from the ultraviolet to the microwave. Appl Opt 1984;23:1206–25.
[21] Bohren CF, Huffman DR. Absorption and scattering of light by small particles. New York: Wiley; 1983.
[22] Baran AJ, Yang P, Havemann S. Calculation of the single-scattering properties of randomly oriented hexagonal ice columns: a comparison of the *T*-matrix and the finite-difference time-domain methods. Appl Opt 2001;40:4376–86.